Pressure and Free Flight Time Effects on Glow Discharge Characteristics

F. Bouanaka
L.M.I, Département d'Electronique,
Université Constantine 1, Route
d'Ain El Bey, 2500 Constantine,
Algérie

S. Rebiai
L.M.I, Département d'Electronique,
Université Constantine 1, Route
d'Ain El Bey, 2500 Constantine,
Algérie

ABSTRACT
In this work, a model for a DC glow discharge at low pressure, used in many applications has been developed. This model allows the determination of plasma characteristics distributions in 2D geometry. The proposed theoretical model is applied to collisional argon plasma at low pressure in a reactor consisting of two plane parallel electrodes where the cathode is heated to a voltage of -250 V. The proposed code is based on solving the continuity equation coupled with Poisson's equation and electrons mean energy's equation. The particles trajectories simulation requires the knowledge of all collisional processes through their collision cross sections. The probability of collision during a free flight time can not be known without performing integrations of non-analytical cross sections. The proposed solution to this problem consists in the application of the "null collision" concept. The simulation results are shown in terms of spatial distribution of charged particles, potential, electric field, electrons energy and velocity. The study of the pressure (0.1-1Torr) and the free flight time ($5.11x10^{-9}$ to $1.46\ x10^{-7}$s) effect, on the plasma characteristics, confirms the validity of this model

Keywords
DC glow discharge, Argon plasma, modeling, charged particles, plasma potential, electron energy.

1. INTRODUCTION
Low pressure plasma technology provides several varieties of applications in micro-electronic industry and materials surfaces processing. There have been recent interests in the area of glow discharge plasmas applications, such as etching, semiconductor wafer processing, treatment of fibrous materials and surface modification by deposition of diamond films [1, 2].
DC glow discharges in the low-pressure regime have long been used for gas lasers and fluorescent lamps. DC discharges are an attractive field to study because the solution is time independent.
The low pressure plasma discharges can produce active chemical species at low temperatures. The numerical simulation of these discharges is a powerful means of physical phenomena investigation. It provides detailed information on complex systems to which the analytical methods of calculation are powerless. It provides as well access to physical parameters often inaccessible to the experiment.
The modeling of a plasma discharge is to determine the kinetics of neutral and charged particles by integrating all mechanisms of collisions that could occur in the gas [3]. Furthermore, plasma modeling has become a valuable tool to understand the plasma physics and has contributed to develop efficient plasma reactors [4, 5]. This was made possible by the development of simplified models and the selection of appropriate simulation techniques [3]. Fluid models, particle (PIC-MC) and hybrid techniques are commonly used for numerical simulation of plasmas at low temperatures [6- 8].
In particular, argon is used as plasma gas in plasma emission spectrometer (ICP) [9] and as a carrier gas in plasma process. It's one of the most noble gases used for plasma surfaces treatment [10, 11]. Moreover, modeling argon plasma is still relevant, because of the simplicity of the chemical reactions that occur in the discharge, in order to test the different models developed with the aim of getting more models effective [12, 13]. In this work, we focus on the modeling of low pressure argon DC discharge plasma. The model enable a better understanding and optimizing technological processes based on the use of cold plasmas in industry. This study is important because it allows a description of system particles evolution under the influence of applied electric field in a two-dimensional geometry. This configuration (unlike the one-dimensional model) allows the consideration of the radial expansion of the landfill, which is a more realistic situation that describes the electrical behavior of landfills [14, 15]. Moreover, from Ref [15], 1D model gives satisfactory accuracy only if the tube radius is larger than the length of the discharge volume.
In case of low-pressure, the simulation of particles trajectories requires the knowledge of all collision processes through their collision cross sections. The probability of a collision during the free flight time (time between successive collisions) can not be known without performing integrations of non-analytical cross sections. One solution to this problem is to apply the concept of "null collision" (concept proposed in this work). This technique involves the introduction of a fictive collision cross section making the total collision frequency constant [16-18].
The proposed model was established using MATLAB, which provides various profiles of plasma characteristics. The aim of this study is to simulate the distributions of charged particles, active species in electric discharge, potential, electric field, electron energy and the electrons velocity of monatomic gas (Argon) created in DC discharge using two-dimensional geometry. To confirm the validity of the model, the effects of the pressure (0.1 Torr-1 Torr) and time of free flight (5.11×10^{-9} to 1.46×10^{-7} s) on these distributions have been studied.

2. PROPOSED MODEL AND SYSTEM OF EQUATIONS

Before presenting the mathematical model developed in this article, it important to note that the phases of discharges studied has at most a few tens of nanoseconds. As the degree of ionization is low and only the densities of charged species are influenced by the discharge, we can consider that the neutrals are inert. So, we have been interested in the transport of charged species, which is partly governed by the total electric field.

Our model is particle type, based on solving the continuity and momentum transfer equations for electrons and positive ions. These equations are coupled with Poisson's equation and the mean energy equation. Thus, the model is simple consisting only of electrons and positive ions Ar^+. In a 2D geometry, the model can be governed by the following system of equations:

-transport equations:

$$\frac{\partial \mathrm{n}_\alpha}{\partial \mathrm{t}} + \frac{\partial \Gamma_\alpha}{\partial \mathrm{r}} = S_\alpha \qquad (1)$$

Where n_α is the particle density, Γ_α the particle flux density and S_α the source term accounting for the effective creation.

The flux of particles, with index α, can be calculated from diffusion-drift expression:

$$\text{For } \alpha = \text{e, i} \begin{cases} \Gamma_e = n_e V_e = -n_e \mu_e E - D_e \dfrac{\partial n_e}{\partial r} \\ \Gamma_i = n_i V_i = n_i \mu_i E - D_i \dfrac{\partial n_i}{\partial r} \end{cases} \qquad (2)$$

Where E is the electric field, *V* the convective velocity, μ and D the mobility and the diffusion coefficient, respectively. Mobility and diffusion coefficient of particles (electron and ion) are approximated by constant parameters, and given by the following expression:

$$D_{e,i} / \mu_{e,i} = k_B T_{e,i} / e \qquad (3)$$

With k_B is the Boltzmann constant, e the elementary charge and $T_{e,i}$ the particles temperature.

- Energy equation for electrons is given by [16]:

$$\frac{\partial n_\varepsilon}{\partial t} + \nabla[n_\varepsilon .(\mu_\varepsilon .E) - D_\varepsilon .\nabla n_\varepsilon] + \Gamma_e .E = S_\varepsilon \qquad (4)$$

Where $n_\varepsilon = <\varepsilon> n_e$ is the energy density, S_ε the source function for electron energy. In this expression, energy transport coefficients are related to particle transport coefficients via:

$$\mu_\varepsilon = (5/3).\mu_e , \qquad D_\varepsilon = (5/3).D_e \qquad (5)$$

- Electric potential profile V from Poisson's equation:

$$\varepsilon_0 \nabla^2 V = -e(n_i - n_e) \qquad (6)$$

Where ε_0 is the vacuum permittivity.

In this section, we describe in detail how the path of an individual electron is simulated. Firstly, we use the hypothesis of weakly ionized gas, taking into account electron-neutral collisions. The monatomic gas processed in this simulation is the argon whose interaction with other elements is very difficult making it useful as carrier gas in sputtering and deposition techniques of thin films. We consider the chemical reactions shown below [12, 19]:

(1) Direct ionization : $Ar + e \rightarrow Ar^+ + 2e$ ΔE =15.8 ev

(2) Stepwise ionization: $2Ar^* \rightarrow e + Ar^+ + Ar$ ΔE = 4.4 ev

(3) Penning ionization: $e + Ar^* \rightarrow 2e + Ar^+$ ΔE = -

Where, ΔE is the electron energy lost in reactions.

Source term S_α in equation (1) is determined by direct, stepwise and penning ionization processes:

$$S_e = S_i = \mathrm{n_e}\, \mathrm{N_g}\, \mathrm{k_i} \qquad (7)$$

Here, N_g denotes the gas density and k_i the reaction ionization constant.

The source function for electron energy loss is obtained by summing the collisional energy loss over all reactions:

$$S_\varepsilon = \sum_{i=1}^{3} k_i .N_g .n_e \Delta E_i \qquad (8)$$

The simulation of the charged particles trajectories requires knowledge of all collisional processes, through their collision cross sections. The probability of such a collision during a time between successive collisions can not be known without making non-analytical integrations of the cross sections, which requires computation time consuming. In our work, the collision treatment is based on the concept of "null collision" by adding a fictive collision chosen to make the total frequency of collisions always constant and to optimize computation time [20]:

$$\nu_{Tot} = \nu_T + \nu_{null} = Cte \qquad (9)$$

In this case, the time of free flight linked to the law of probability is given by the equation:

$$t_{vol} = -\frac{1}{\nu_{tot}} \ln(R_{vol}) \qquad (10)$$

Where R_{vol} is a random number uniformly distributed between 0 and 1. Throughout the mean free path t_{vol} , the electron moves freely. Its path is calculated by integrating the equation of motion:

$$\left.\begin{array}{l} \dfrac{dv}{dt} = \dfrac{-e}{m_e} E(x) \\ \dfrac{dr}{dt} = v \end{array}\right\} \quad \frac{d^2 r}{dt^2} = \frac{-e}{m_e} E(x) \qquad (11)$$

So, when t_{vol} is calculated using relation (10), the time step $dt = t_{vol}/100$ is determined and all parameters of the discharge are calculated. In this case, we can evaluate de electron velocity *v* in the inter electrodes space by the use of the relation (11).

3. NUMERICAL TREATMENT

The system consisting of transport equations and electrons energy coupled with Poisson's equation can not be solved analytically. It is therefore necessary to be resolved with one of the several numerical methods used for solving the Partial Differential Equation (PDE). Our elaborated model was based on finites differences method and solved by MATLAB software. Solving equations of transport, energy and electric field required their temporal spatial discretizations. 2D mesh was used to determine the points where densities of species, electron energy and electric field will be calculated (see Figure1).

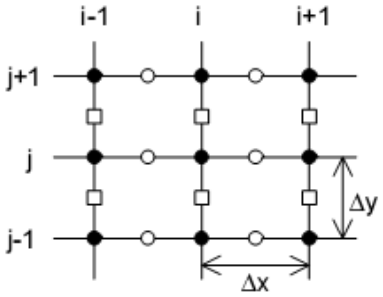

Fig 1: Spatial grid used for the numerical solution of system of equations.

The mesh steps considered in our calculation are Δx= 0,03cm and Δy= 0, 03 cm verifying the following condition [21]:

$$\lambda_D / \Delta x \geq 2 \text{ and } \lambda_D / \Delta y \geq 2$$

Where λ_D is electronic Debye length calculated with an initial density of electrons.

Poisson's equation is solved on the entire grid, except inside electrode areas.

The flux of ions, electrons and energy are discretized by finite difference method using the Sharfetter-Gummel exponential scheme for numerical discretization of the flux. The system of equations is linearized and integrated implicitly.

$$\nabla\Gamma_{i,j} = \frac{\Gamma_{i+1/2,j} - \Gamma_{i-1/2,j}}{\Delta x} + \frac{\Gamma_{i,j+1/2} - \Gamma_{i,j-1/2}}{\Delta y} \quad (12)$$

To integrate motion equation, we used the Leap-frog method [22]. In finite differences method, the motion equations are written as follows:

$$\begin{aligned} v(i+1/2) &= v(i-1/2) - \frac{\Delta t.e}{2m_e}(E(x_i) + E(x_{i+1})) \\ x(i+1) &= x(i) + v(i).\Delta t - \frac{\Delta t^2}{2.m_e}E(x_i) \end{aligned} \quad (13)$$

4. BOUNDARY CONDITIONS

The numerical resolution of the equations in 2D model requires the introduction of initial and boundary conditions. According to reported work in literature [23, 24], the numerical solution of the partial differential equation depends essentially on the nature of these conditions and on the integration steps. It is known that the validity of our numerical results is strictly bound with these physical, electrical and numerical conditions (see Figure 2).

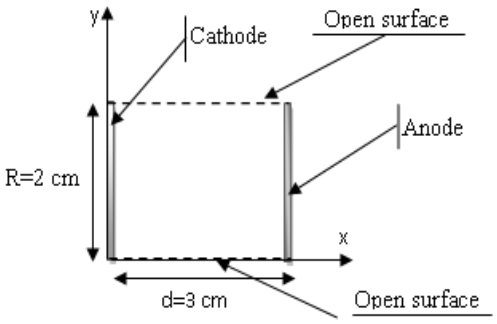

Fig 2: Schematic representation of the boundaries conditions used in our model.

The boundary conditions used in the simulation are assumed as follows:

- For the electron density and electron energy density at the anode.

$$\Gamma_e = \frac{1}{4}v_e n_e \qquad \Gamma_\varepsilon = \frac{1}{2}v_e \varepsilon, \text{ where } \varepsilon = \frac{3}{2}k_B T_e$$

While at the cathode $\Gamma_e = \frac{1}{4}v_e n_e - \gamma\Gamma_i$,

Where v_e is the thermal velocity given by:

$$v_e = \sqrt{8k_B T_e / \pi m_e}$$

And electron energy at the cathode is given by:

$$\Gamma_\varepsilon = \frac{1}{2}v_e \varepsilon - 2k_B T_e \gamma\Gamma_i$$

Where γ is the secondary electron emission coefficient.

- Boundary condition for ions at the anode and the cathode are given by:

$$\Gamma_i = \frac{1}{4}v_i n_i + \alpha n_i \mu_i (\hat{n}.E)$$

Here the ion thermal velocity is given by:

$$v_i = \sqrt{8k_B T_i / \pi m_i}$$

$\hat{n}$ is the normal unit vector pointing towards the surface, and α is a switching function (0 or 1) depending on positive ion drift direction at surface: α = 1 if $\hat{n}.E > 0$ and α=0 otherwise.

- At the open surface, a set of Neumann symmetry boundary conditions is imposed. This corresponds to

assume a zero axial derivative for charged particle density and energy flux:

$$\frac{\partial \Gamma_e}{\partial x} = 0,\ \frac{\partial \Gamma_i}{\partial x} = 0 \ \ and \ \frac{\partial \Gamma_\varepsilon}{\partial y} = 0$$

- For electric potential, we set V= -250 V at the cathode and V= 0 at the anode while at the open surface we have: $\frac{\partial V}{\partial y} = 0$

5. RESULTS AND DISCUSSION

The results are given for a DC glow discharge at low pressure between two plane parallel electrodes in argon at a pressure of 1Torr and an inter-electrode distance of 3 cm. The simulations are carried out for T_i = 300 K = T_g (gas temperature) and particle transport coefficients (Diffusion and mobility) approximated by constants. In our model we take γ = 0.03 at the cathode and γ = 0 at all other surfaces. The two-dimensional distribution of charged particles density, electric field and average energy flow of electrons are presented to illustrate the behavior of the discharge in the DC regime.

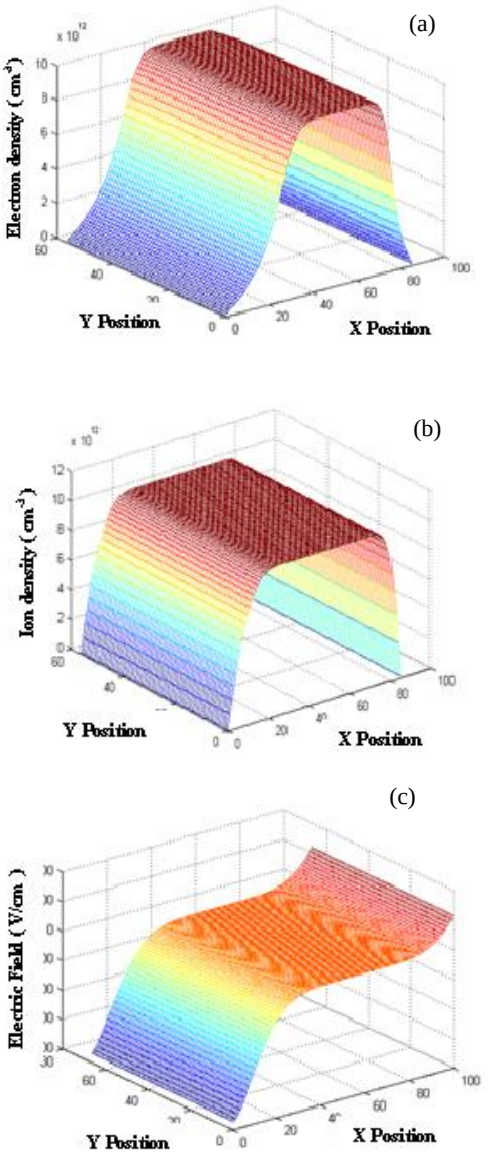

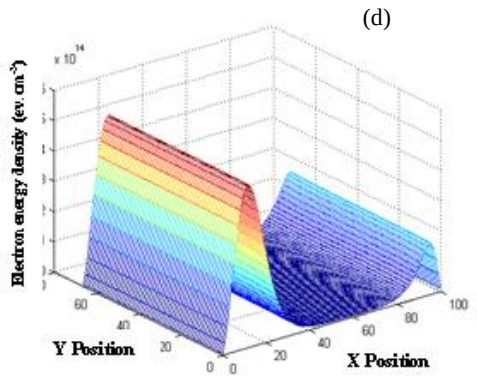

Fig 3: (a) electrons densities, (b) ions densities, (c) electric field and, (d) Electron energy density.

Figure 3 (a) and Figure 3 (b) present the spatial distribution of electron and ion densities in the landfill for a free flight time of 4.99 10^{-8} s. The results clearly show the presence of three distinct regions of the discharge. The maximum density of charged species in the gap was about 10^{13} cm^{-3}. Figure 3(c) shows the spatial distribution of the electric field. In the cathode sheath, the field variation is linear because of potential fall. The field is zero in the plasma zone, where the potential is flat.

Figure 3 (d) shows the 2D profile of electron energy density for DC discharge in Argon plasma. This profile is only important within the sheaths where it presents two maxima. This is an effect of the strong intensity of the electric field in these regions where the electrons temperature is high.

These results are compared with the simulation carried for p = 1Torr, V = 250 V and L = 1 cm, in ref [13] for argon glow discharge with a simple fluid model, an extended fluid model, where electron transport coefficients and the rates of the electron-induced plasma chemical reactions are calculated as functions of the mean electron energy and the two new models with a nonlocal ionization source. The plasma electron density obtained by our simulation (around 10^{13} cm^{-3}) for "pL = 3 Torr.cm" seems consistent with the new models where plasma electron density is about 10^{11} to 10^{12} cm^{-3}, contrary to the extended fluid model where the electron density is underestimated.

According to the conditions used at open surfaces, the various characteristics illustrated in figure 3 have a radial profile uniform in all the bulk of the discharge. Thus, in what follows, we just descript the axial simulation results.

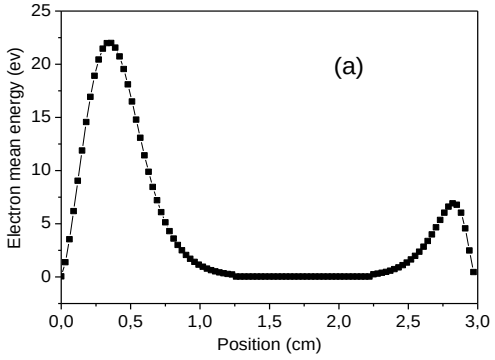

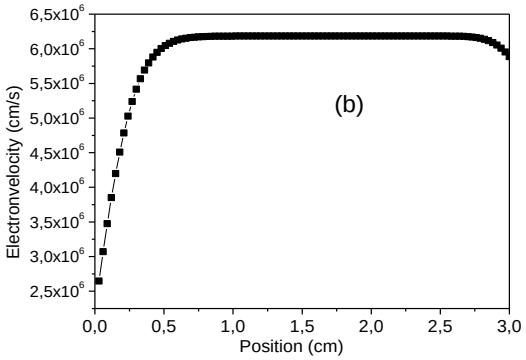

Fig 4: Axial distribution of: (a) the electron mean energy, (b) the electron velocity.

The axial distribution of electron mean energy is shown in Figure 4(a). The electron energy at the edge of the cathode sheath is very high due to the energy gained from the sheath electric field. The drop in electron energy after the sheath and in the plasma region is due to the energy loss and heat conduction. This region is characterized by a low mean energy of about 0.04eV**.**

The max value of the mean energy of electrons in the cathode sheath is about 22 eV. It corresponds to an electron temperature of 14.66 eV. This value is close to that obtained by the two models of ref [13] but lower than that obtained in ref [12] by fluid models using the software COMSOL Multiphysics for "p.L = 3 Torr.cm".

Figure 4(b) shows the axial distribution of the electrons velocity. We noticed that at the cathode, the velocity is equal to the initial rate (start condition), and then the change in velocity follows an increase in the sheath. The electron velocity is practically constant at about 6.2×10^6 cm / s in the plasma zone where the electric field is zero and this speed is lower near the anode.

5.1 Influence of gas pressure

To validate our model, we simulate the variations of the potential profile, electric field, electrons density at the sheath, electrons mean energy and electrons speed when the pressure varies from 0.1 Torr to 1Torr. The results are illustrated in Figure 5(a, b, c and d).

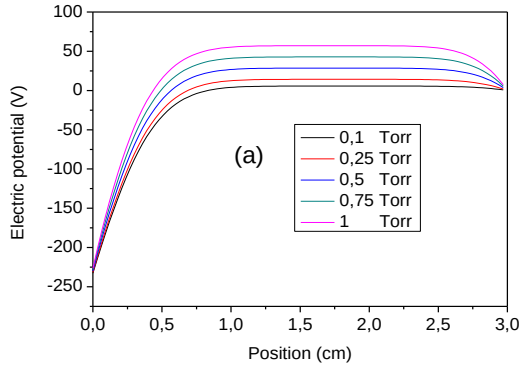

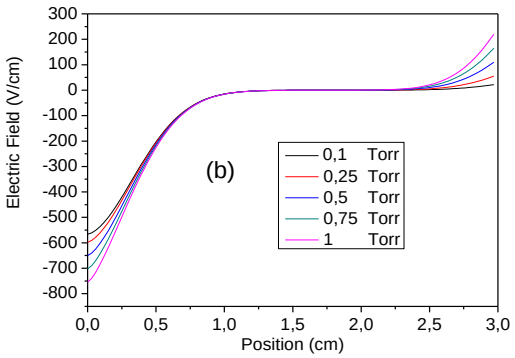

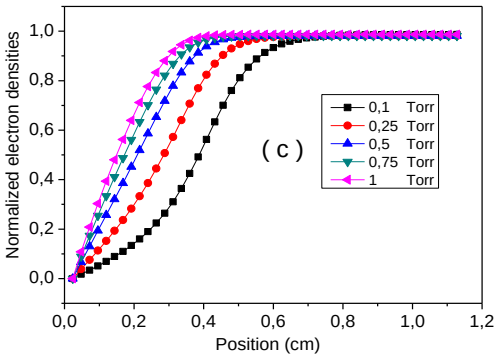

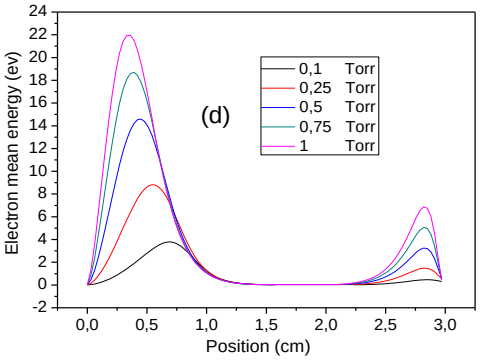

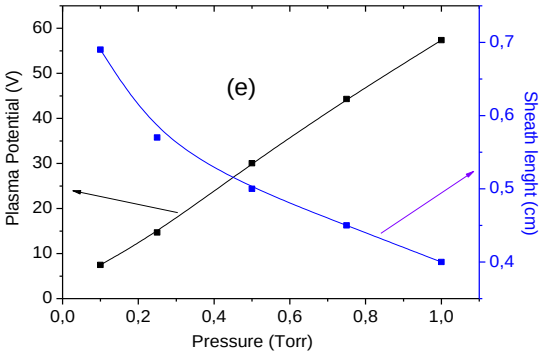

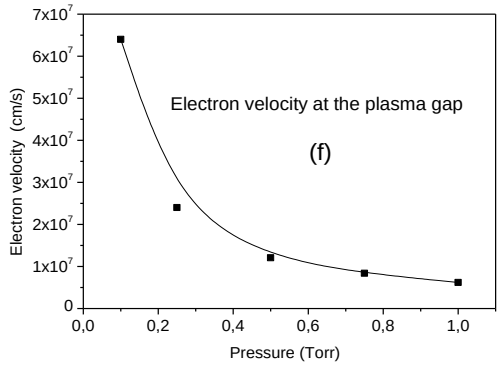

Fig 5: Effect of pressure: (a) Profile of the potential, (b) Electric field, (c) Normalized distribution of electrons density in the area of the cathode sheath, (d) Electron mean energy, (e) Velocity of electrons at the plasma gap, and (f) plasma potential and sheath length.

Figure 5 (a) to Figure 5 (d) present the plasma characteristics calculated for reactor gas pressure varying from 0.1 to 1Torr. The simulation results are given with an increment time (dt) of 3.98×10^{-11} s. The obtained curves show clearly that the effect of increased pressure induces an increase in the plasma potential V_p with a simultaneous narrowing of the sheath thickness (see Figure 5(e)) and an increase of the electric field and the mean electron energy in the sheaths. These results confirm that the energy which is transferred to the electron scales well with the Electric field [25].

According to Figure 5(f), we note that when the working pressure increases the rate of electrons in the positive column decreases. The rate falls from 6.4×10^{7} cm/s at a pressure of 0.1 Torr to the value of 6.2×10^{6} cm/s at a pressure of 1 Torr.

5.2 Influence of the free flight time (t_{vol})

The presented model has been tested for several values of free flight time. The simulation was carried out for reactor pressure of about 1 Torr. Figure 6 shows the variation of electron density in the space between electrodes as a function of later parameter. The curves show a narrowing of the plasma zone with an increasing of the t_{Vol}. Effectively, this increase of free flight time is directly related to a reduction in the number of collisions between particles which produces a diminution of the plasma zone.

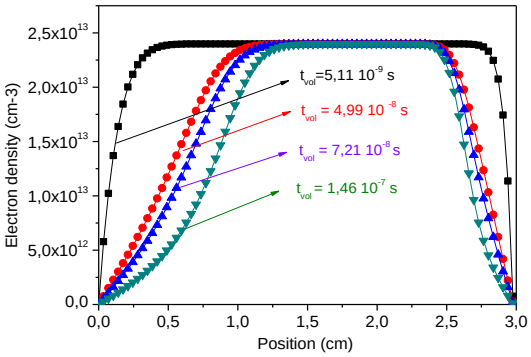

Fig 6: The variation of the electrons density in the space between electrodes as a function of free flight time.

We have presented in Figure 7 the spatial evolution of the mean energy of electrons for different values of free flight time. The obtained curves clearly show the presence at the sheaths of two energy maxima (Emax1 and Emax2) whose position and intensity change with time of free flight t_{vol}.

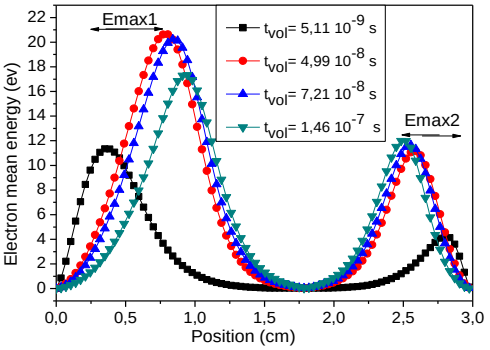

Fig 7: The spatial evolution of the mean energy of electrons for different values of free flight time.

Emax2 intensity increases with the value of t_{vol}. Indeed, the most important time of free flight values correspond to fewer collisions, which is less energy loss (see Figure 8).

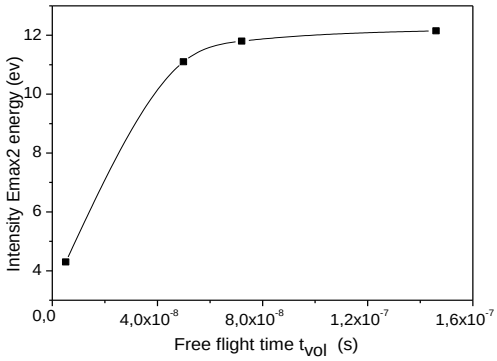

Fig 8: The intensity of Emax2 for different values of free flight time.

Full exploitation of Fig. 7 and Fig. 8 leads to the evaluation of the sheath width and energy maximum position Emax1 (compared to the cathode) with free flight time. The curves obtained show a similar increase of the two parameters with the free flight time t_{vol} (see Fig. 9).

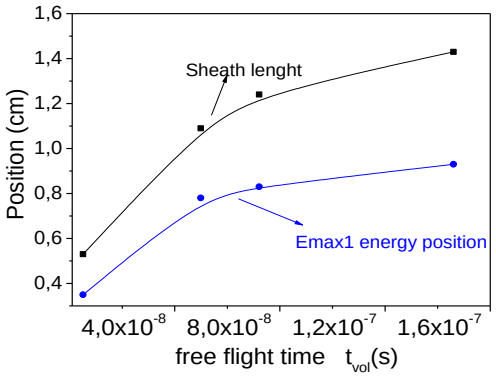

Fig 9: The length of the sheath and the position of the maximum energy Emax1 for different values of free flight time.

6. CONCLUSIONS

In this paper, simulation results by considering a model of a DC plasma discharge at low pressure in argon for a two-dimensional configuration and taking in consideration the concept of null collision have been presented. This configuration allowed the consideration of the glow discharge properties more realistic. The results are presented in terms of spatial variation of charge density, electric field, average energy of electrons and electron velocity. We have used this simulation to study the effect of working pressure on the plasma characteristics. The results indicate that the collisional proposed model provides a good agreement with plasma characteristics for pressure ranging between 0.1 and 1 Torr. Moreover, we have correlated the increase of the free flight time from 5.11×10^{-9} to 1.46×10^{-7}s with the simultaneously increase of the sheaths thickness and the value of maximum of electrons mean energy.

7. REFERENCES

[1] M. Moradshanhi, T. Tavakoli, S. Amiri et al, Surface and Coatings Technology, 201(3), 567 (2006).

[2] M. A. Lieberman, A. J. Lichtenberg, principles of plasma discharges and materials processing, (John Wiley, New York), 1994.

[3] D. Hash, D. Bose, and T. R.Govindan et al, Journal of applied physic, Vol. 93, N^{O} 10, pp (6284-6290), 2003.

[4] T. E. Nitschke and D. B. Graves; Journal of applied physic, Vol. 76, N^{o} 10, pp (5646-5660), 15 November 1994.

[5] A. Bogaerts, R. Gijbels, Science Direct, Vol. 69, pp (37–52), 2003

[6] H. C .Kim1, F .Iza, and S .S Yang, et al**,** J. Phys. D: Appl. Phys. Vol 38, pp (283–301), (2005).

[7] P. Bartos, R. Hrach, P. J. nek, Science Direct, Vacuum 82 (2008) 220–223

[8] E. Gogolides, H. Sawin, Journal of applied physic, Vol. 72,N^{O} 9, 1992, pp (3971-3987).

[9] S. Iordanova and I.Koleva, Spectrochimica Acta part B, 62 (2007), 344-356.

[10] R. Kawakami and T. Inaoka, ELSEVIER, Vacuum, 83(2009), 490–492.

[11] D.Tashima, A. Sakamoto, and M. Taniguchi, et al, ELSEVIER, Vacuum, 83 (2009) 695–698

[12] I. Rafatov, E. A. Bogdanov and A. A. Kudryavtsev, Phys. Plasmas 19, V. 033502 (2012)

[13] I. Rafatov, E. A. Bogdanov and A. A. Kudryavtsev, Phys. Plasmas 19, V. 093503 (2012)

[14] R. R. Arslanbekov and V. I. Kolobov, J. Phys. D: Appl. Phys., v. 36, p.2986, 2003.

[15] E. A. Bogdanov, S. F. Adams, V. I. Demidov, A. A. Kudryavtsev and J. M. Williamson, Phys. Plasmas, v.17, N10, 103502(1-11), 2010.

[16] A. Bogaerts, R. Gijbels, Spectrochimica Acta Part B. 57, (2002) 1071.

[17] S. Roy and B. P. Pandey**,** Physics of plasmas**,** 10(2003), 2578.

[18] I. Denysenko, K. Ostrikov, and P.P. Rutkevych et al , Computational Materials Science, 30 (2004), 303

[19] N. Balcon, G.J.M Hagelaar and J.P.Boeuf, IEEE, Trans, Plasma Sci. 36 2782-7(2008)

[20] H.R. Skullerud, J. Appl. Phys, D2, 1567-1563 (1968).

[21] Vladimir, V. Serikov, and S. Kawamoto, et al, IEEE transactions on plasma science, vol. 27, no. 5, October 1999

[22] J.P. Nougier, Méthode de calcul numérique, Hermes Science 2001.

[23] A. Salabas, G. Gousset, L.L.Alves**,** Science Direct, Vacuum, 69 (2003), pp 213-219.

[24] J.P. Bœuf and L.C. Pitchford, Physical Review E, Volume 51, Number2, February 1995.

[25] Gerhard Franz, Low Pressure Plasmas and Microstructuring Technology, Springer-Verlag Berlin Heidelberg 2009